Interferometric measurement of the tip oscillation amplitude in apertureless near-field optical microscopy

Pietro Giuseppe Gucciardi[a)]
CNR-Istituto per i Processi Chimico-Fisici, Via La Farina 237, I-98123 Messina, Italy

Guillaume Bachelier and Adnen Mlayah
Laboratoire de Physique des Solides, Université Paul Sabatier, Bât. 3R1b2,118, Route de Narbonne, F-31062 Toulouse, France

Maria Allegrini
INFM, Dipartimento di Fisica, Università di Pisa, Via Buonarroti 2, I-56126 Pisa, Italy

We have implemented an optical homodyne interferometer to measure the tip oscillation amplitude in apertureless near-field optical microscopy. The setup is fully embedded in the microscope's design, avoiding the presence of external arms. Our method is based on the synchronous detection of the interference between the fields reflected by the tip and a glass sample surface, while scanning the tip–sample distance over a few wavelengths. With the help of a simple model, we show how the different interference terms arising at frequencies multiple of the tip oscillation can be exploited to easily achieve sub-Ångstrom resolution. © *2005 American Institute of Physics.* [DOI: 10.1063/1.1866912]

Apertureless scanning near-field optical microscopy (a-SNOM) has pushed the optical resolution below 10 nm.[1,2] The a-SNOM setup is based on atomic force microscopy (AFM) working in the tapping mode,[3] implemented for what concerns the optical excitation and the collection of the scattered light. A metallized tip, located at the edge of the cantilever beam, oscillates orthogonally to the sample surface with an amplitude a_0 ranging from a few nanometers (soft tapping or noncontact) to a few tens of nanometers (hard tapping). The tip oscillation is detected either optically,[4] or by piezoelectric means after gluing it perpendicular to a quartz tuning-fork.[5] The tip oscillation amplitude is a parameter of relevant importance for different reasons: regarding the imaging capabilities, the tip modulation serves as a band-pass filter of the spatial frequencies associated with the oscillation amplitude,[6] acting as an effective tip sharpening;[7] tip-induced surface plasmon modes can produce an enhancement of the optical near-fields, and the resonance energy notably shifts with the tip–sample distance;[8] in nanolithography, increasing a_0 leads to a reduced time interval into which the evanescent near fields are in proximity of the photosensitive surface, with consequences on the dimensions of the nanostructures so produced.[9] The most widely used method to measure the vibration of AFM or SNOM probes exploits an external differential interferometer setup[10–12] placed at close distance from the probe (a few mm). In this scheme, the laser beam is split into a probe and a reference beam. Once recombined onto the detector, the two beams provide a signal proportional to the oscillation amplitude with sub-Ångstrom accuracy. Placing a further interferometer in proximity of an a-SNOM tip can be troublesome, both for what concerns the lack of space (the collection optics needs to be placed close to the probe), and the mechanical stability. In this paper we show the implementation of an interferometer, similar to the Mirau configuration adopted by optical profilers.[13] It exploits the optical elements embedded in a-SNOM which employs lock-in detection techniques at different harmonics for fast and precise measurements of a_0.

The experimental setup is sketched in Fig. 1. The tip, glued to a tuning fork (TF), is oscillated at resonance ($f_0 \sim 32.5$ kHz) by a dither piezo driven by a function generator (V1). The probe beam (E_F) is provided by a HeNe laser ($\lambda = 632.8$ nm), coupled to a single mode optical fiber, whose output is collimated, reflected by a 50% beamsplitter (BS1), and, after passing a further beamsplitter (BS2), focused to one of the TF prongs, beside the tip, by means of a lens (L, $f = 8$ mm). The reference beam originates from the back-reflection (E_S) of BS2, which is mounted on a piezo-tube whose vertical axis is driven by a linear voltage ramp (V2). Finally, part of the light impinging on L is back-reflected (E_L) and reaches the photomultiplier (PMT), interfering with E_F and E_S. The PMT output is split and sent both to a lock-in amplifier referenced to the TF oscillation, and to a low-pass filter ($f_c = 1.6$ kHz $\ll f_0$). A digital oscilloscope is used to acquire simultaneously the lock-in signal S_n demodulated at the nth harmonic, the low-passed optical signal S_0, and the driving piezo voltage, during the z-scan of BS2. Another oscilloscope, preceded by an I/V converter ($G = 21.76$ mV/nA), is used to measure the current generated by the TF.[14]

Let us call $a(t) = a_0 \cos \omega t$ the tip oscillation ($\omega = 2\pi f_0$), and l_0 the average distance between the oscillating tip and the fixed lens L. The position of BS2 will be $z(t) = z_0 + \Delta z(t)$, where z_0 is the TF-BS2 average distance, and $\Delta z(t)$ the z-scan amplitude. The signal measured by the detector will be proportional to

[a)]Electronic mail: gucciardi@me.cnr.it
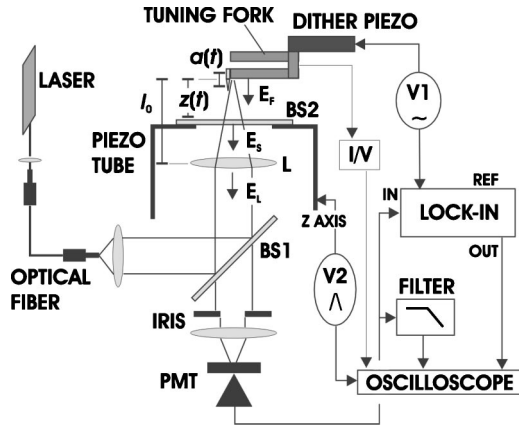
FIG. 1. Sketch of the experimental setup.

FIG. 2. dc interference patterns related to (a) the L1-BS2 assembly, (b) the TF-BS2-L1 system. The interference signal demodulated in-phase with the TF oscillation at the first (c) and second (d) harmonic, carry information on the TF oscillation amplitude. The black symbols correspond to the experimental values, the grey lines are the fits.

$$I = |E_F + E_S + E_L|^2$$

$$= C + B_{FS} \cos[4\pi/\lambda \cdot (z(t) + a_0 \cos \omega t)]$$

$$+ B_{LF} \cos[4\pi/\lambda \cdot (l_0 + a_0 \cos \omega t)]$$

$$+ B_{LS} \cos[4\pi/\lambda \cdot (l_0 - z(t))], \tag{1}$$

where $C = |E_F|^2 + |E_S|^2 + |E_L|^2$, $B_{FS} = 2|E_F E_S|$, $B_{LF} = 2|E_L E_F|$, and $B_{LS} = 2|E_L E_S|$.

In the small oscillations approximation $(4\pi/\lambda)a_0 \ll 2\pi$, i.e., $a_0 \ll \lambda/2$ (well verified in a-SNOM operation), and high oscillation frequency $[f_0 \gg 1/\lambda \cdot d(\Delta z)/dt]$, we expand Eq. (1) in power series of $(4\pi/\lambda)a_0 \cos \omega t$, up to the fourth order. Expanding $(\cos \omega t)^n$ in terms of $\cos(n\omega t)$, after recombining the harmonic terms, we can write $I = \Sigma_n I_n \cos(n\omega t)$. The first three terms will be

$$I_0 = C + C_0 \cos(\phi_0) + A_0 \cos[\phi_2 + 4\pi/\lambda \cdot \Delta z(t)]$$

$$+ B_{LS} \cos[\phi_1 - 4\pi/\lambda \cdot \Delta z(t)], \tag{2}$$

$$I_1 = C_1 \sin(\phi_0) - A_1 \sin[\phi_2 + 4\pi/\lambda \cdot \Delta z(t)], \tag{3}$$

$$I_2 = C_2 \cos(\phi_0) - A_2 \cos[\phi_2 + 4\pi/\lambda \cdot \Delta z(t)], \tag{4}$$

where

$$A_0 = [1 - 4(a_0\pi/\lambda)^2 + 4(a_0\pi/\lambda)^4] \cdot B_{SF}, \tag{5}$$

$$A_1 = 4(a_0\pi/\lambda)[1 - 2(a_0\pi/\lambda)] \cdot B_{SF}, \tag{6}$$

$$A_2 = 4(a_0\pi/\lambda)^2[1 - 4/3 \cdot (a_0\pi/\lambda)^2] \cdot B_{SF}, \tag{7}$$

with $\phi_0 = 4\pi l_0/\lambda$, $\phi_1 = (4\pi/\lambda)(l_0 - z_0)$, $\phi_2 = (4\pi/\lambda)z_0$, and C_n ($\propto B_{LF}$) independent from Δz.

The key point here is that an optical signal is expected at every harmonic order, oscillating with Δz, whose amplitude scales as $(a_0\pi/\lambda)^n$. Since the L-BS2 distance does not oscillate at the tip frequency, the corresponding interference term ($\propto B_{LS}$) only contributes to I_0, not to the harmonics. Therefore, such term can be singled out by pushing the TF away from the optical path and carrying out a z-scan of BS2. The measured signals S_n ($\propto I_n$) carry information about a_0. The presence of the B_{LS} and C_n terms, however, prevent from calculating a_0 from simple ratios S_n/S_k. We have first to determine the amplitudes A_n by fitting the experimental curves $S_n(\Delta z)$, and finally evaluate a_0 from the ratios A_n/A_k. First of all, we characterize the L-BS2 interference, removing the TF

and acquiring $S_0(\Delta z)$ [Fig. 2(a), black symbols] during a z-scan. From a fit [Fig. 2(a), grey line] we obtain the values of $B_{LS}(\sim 0.4 \text{ mV})$ and ϕ_1, which will be used as known parameters in the following. We now introduce the TF. Applying a dither voltage amplitude $V = 0.6$ V (resulting in an oscillation of ~ 0.35 nm of the dither-piezo) the TF piezo-current amplitude is $I = 8.73$ nA. The $S_0(\Delta z)$ curve [Fig. 2(b)] features a remarkable increase of the signal due to the good reflectivity of the TF. In fact, a fit of S_0 using Eq. (2) leads to a value $A_0 \approx 16 \cdot B_{LS} \cong 6.45$ mV. The uncertainty on A_0 (~ 0.16 mV, corresponding to $\sim 2.5\%$) comes from the fit, which takes into account also the uncertainty (± 0.1 mV) associated with the B_{LS} term. We note that, even disregarding such contribution, the maximum error we could commit on A_0 is of the order of B_{LS}, i.e., $\sim 6\%$. Simultaneously with S_0, we acquire the first harmonic in-phase demodulated signal S_1 [Fig. 2(c), black symbols]. The z-scan is carried out in $T = 6.25$ s and the lock-in integration time set to $\tau = 200$ ms. We note the $\pi/2$ phase shift between S_0 and S_1, predicted by Eqs. (2) and (3). A fit using Eq. (3), [Fig. 2(c), grey line] gives $A_1 \cong 0.08 A_0$ with an error of $\sim 1.5\%$ (mainly due to electronic noise). Subsequently we acquire the demodulated in-phase signal at the second harmonic S_2 [Fig. 2(d), black symbols], showing the π phase shift with respect to S_0. A fit using Eq. (4) yields $A_2 \cong 1.8 \cdot 10^{-3} A_0$ with an error of $\sim 1.5\%$ [Fig. 2(d), grey line]. The ratios A_n/A_k are polynomial functions of a_0 that numerically solved give $a_0(A_1/A_0) = 4.1 \pm 0.2$ nm, $a_0(A_2/A_0) = 4.2 \pm 0.2$ nm, $a_0(A_2/A_1) = 4.3 \pm 0.1$ nm. The error on a_0 calculated from the ratios involving A_0, mostly suffers of the uncertainty of the term proportional to B_{LS}. Conversely, the determination of a_0 through the harmonics ratio is independent from the L-BS2 interference, decreasing the uncertainty by a factor 2, and proving the advantages of the demodulation at higher harmonics.

Sweeping the dither voltage, we vary a_0 in the $1-10$ nm range. In Fig. 3 we plot the measured values of a_0 against the TF piezo-current. The different symbols refer to the various ratios A_n/A_k used for the calculation (see inset). The values are consistent within the experimental errors (the bars coincide with the symbols). A linear fit provides the TF calibration coefficient $\beta = 0.48 \pm 0.01$ nm/nA, in good agreement
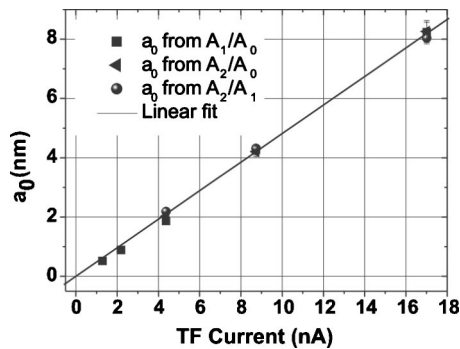
FIG. 3. Plot of the TF oscillation amplitude, calculated from the optical signal demodulated at the different harmonics (see the inset), as a function of the piezo-current delivered by the TF.

with what reported in Ref. 14, measured by means of an external Wollaston-prism interferometer.

S_2 is expected to be a factor $(\pi a_0/\lambda)^2$ smaller than S_0, i.e., $\sim 10^{-4}$ for $a_0 = 1$ nm, while for the first harmonic $S_1/S_0 \sim 2 \cdot 10^{-2}$. This explains why in our case the second harmonic signal resulted too noisy for amplitudes below 2 nm, whereas the first harmonic is perfectly detectable even for subnanometer values of a_0. Figure 4 shows the behavior of $|S_1|$ vs Δz (black symbols) providing, after fitting (grey line), a value $a_0 = 0.50 \pm 0.02$ nm with sub-Ångstrom accuracy. Such a pattern remarkably reproduces the behavior reported in Refs. 2 and 15 for the tip–sample approach curves in the far-field regime, as expected.

The precise determination of a_0 is based on the accuracy of the measurement of the modulation amplitude of the signals S_n. The most important noise sources are represented by electrical noise, and mechanical drifts (mainly thermal), inducing changes of the phases ϕ_n. The latter point, in particular, defines some constraints regarding the mechanical stability of the system. Since S_0 is measured on a T time scale, the drifts of l_0 and $z(t)$ must be much smaller than $\lambda/4\pi \approx 50$ nm within T. This is usually fulfilled by the design commitments in scanning probe microscopy. For what concerns the harmonics, the same considerations are valid. But, in addition, the drifts and thermal-noise Fourier components of l_0 and $z(t)$ at frequency f_0, integrated on a bandwidth
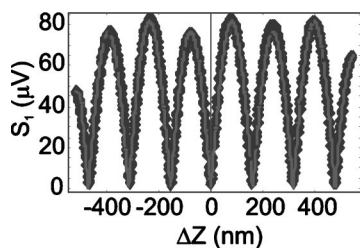
$\Delta f = 1/\tau$, must also be much smaller than a_0. The use of the harmonics for the measurement of a_0 concerns the extraction of small modulations superimposed to a huge S_0 signal. In particular, when scaling a_0 to subnanometer values such a signal can fall below the detector's electronic noise. The harmonic's signals can indeed be enhanced by increasing the light intensity. But saturation of the detector must be prevented, since it would add unphysical nonlinear terms (we measured contributions up to the sixth harmonic), invalidating the measurement. The dynamic range of the detector is thus one of the most important parameters for this technique.

In summary, we have implemented a homodyne Mirautype interferometer to measure the tip oscillation amplitude in a-SNOM. The use of lock-in demodulation at harmonics multiple of the tip oscillation frequency permits to easily achieve sub-Ångstrom sensitivity. The exploitation of the second harmonic signal allows for an increased precision, cutting out the influences of spurious reflections by the focusing optics. Such a method can be applied, more generally, to other scanning probe microscopies in which the tip is vibrated, although a-SNOM is clearly the best target since the optical components are already embedded. Finally, we outline that the presence of components of the optical signal at every harmonic has important consequences (to be fully described elsewhere) for the assessment of the far-field background in a-SNOM imaging based on higher harmonics demodulation.[2,16]

FIG. 4. Plot of the modulus of the first harmonic optical signal (black symbols), leading to an oscillation amplitude of 0.5 nm. The fit (grey line) evidences the different heights of the maxima which are related to the presence of the $C_1 \sin(\phi_0)$ offset evidenced in Eq. (3).

[1] F. Zenhausern, M. P. O'Boyle, and H. K. Wickramasinghe, Appl. Phys. Lett. **65**, 1623 (1994).
[2] R. Hillenbrand and F. Keilmann, Appl. Phys. Lett. **80**, 25 (2002).
[3] C. A. J. Putman, K. O. Van der Werf, B. G. De Grooth, N. F. Van Hulst, and J. Greve, Appl. Phys. Lett. **64**, 2454 (1994).
[4] S. Alexander, L. Hellemans, O. Marti, J. Schneir, V. Elings, P. K. Hansma, M. Longmire, and J. Gurley, J. Appl. Phys. **65**, 164 (1989).
[5] F. J. Giessibl, Appl. Phys. Lett. **73**, 3956 (1998).
[6] P. M. Adam, J. L. Bijeon, G. Viardot, and P. Royer, Opt. Commun. **174**, 91 (2000).
[7] B. Knoll and F. Keilmann, Opt. Commun. **182**, 321 (2000).
[8] J. A. Porto, P. Johansson, S. P. Apell, and T. Lopez-Rios, Phys. Rev. B **67**, 085409 (2003).
[9] R. Bachelot, F. H'Dhili, D. Barchiesi, G. Lerondel, R. Fikri, P. Royer, N. Landraud, J. Peretti, F. Chaput, G. Lampel, J.-P. Boilot, and K. Lahlil, J. Appl. Phys. **94**, 2060 (2003).
[10] Y. Martin, C. C. Williams, and H. K. Wickramasinghe, J. Appl. Phys. **61**, 4723 (1987).
[11] C. Schönenberger and S. F. Alvarado, Rev. Sci. Instrum. **60**, 3131 (1989).
[12] R. Toledo-Crow, P. C. Yang, Y. Chen, and M. Vaez-Iravani, Appl. Phys. Lett. **60**, 2957 (1992).
[13] B. Bushan, J. C. Wyant, and C. Koliopoulos, Appl. Opt. **24**, 1489 (1985).
[14] K. Karrai, in *Le Champ Proche Optique*, edited by D. Courjon and C. Bainier (Springer-Verlag et France Telecom R&D, Paris, 2001).
[15] F. Formanek, Y. De Wild, and L. Aigouy, J. Appl. Phys. **93**, 9548 (2003).
[16] M. Labardi, S. Patané, and M. Allegrini, Appl. Phys. Lett. **77**, 621 (2000).